Influence of interface roughness on excitonic diffusion in semiconductor quantum well

2003 J. Phys.: Condens. Matter 15 8137

(http://iopscience.iop.org/0953-8984/15/47/016)

INSTITUTE OF PHYSICS PUBLISHING JOURNAL OF PHYSICS: CONDENSED MATTER

J. Phys.: Condens. Matter **15** (2003) 8137–8145 PII: S0953-8984(03)66328-9

Influence of interface roughness on excitonic diffusion in semiconductor quantum well

Huijun Tang

Department of Physics, Northern Jiaotong University, Beijing 100044, People's Republic of China

Received 16 July 2003
Published 14 November 2003
Online at stacks.iop.org/JPhysCM/15/8137

Abstract

We report a Monte Carlo investigation on the excitonic diffusion process in semiconductor quantum wells (QW). The rates of interface-roughness scattering and phonon scattering are calculated. By comparing the scattering rates, we find that, in a realistic QW sample with typical well-width and interface quality, the interface-roughness scattering is the dominant mechanism in limiting the diffusivity. Spatiotemporal dynamics of the exciton distribution function are obtained by the simulations and the excitonic diffusivity under different conditions is deduced. We find that the diffusivity increases rapidly with increasing the correlation length of the interface fluctuation and with decreasing the amplitude of the fluctuation. In a typical QW sample, the diffusivity increases exponentially with increasing the width of the well.

1. Introduction

In semiconductors, a photon with suitable energy can excite an electron from the valence band to the conduction band, leaving a hole in the valence band. The Coulomb attraction between the excited electron and the positively charged hole may lead to the formation of a hydrogen-like quasi-particle, called an exciton. In most bulk materials, the binding energy of an exciton is as small as a few millielectronvolts and thus the exciton is stable only under low temperatures. However, in quantum wells (QWs) the confinement along the growth direction significantly enhances the binding energy and thus the stability of excitons. In these structures the excitonic process dominates most of the optical properties even up to room temperature. Due to its fundamental and technological importance, the excitonic process in semiconductor QWs has been extensively studied during the past three decades [1].

Real-space transport describes the movement of excitons inside the sample during its lifetime. In a QW, the movement of excitons along the growth direction is confined by the potential barriers so that the excitonic transport is an in-plane process. On the macroscopic length scale, the in-plane transport of an exciton is well described by diffusion. Such a kind of process in a number of QW structures has been extensively studied by several optical

methods including four-wave mixing [2–4], pump–probe [5–7], time-of-flight [8–10] and photoluminescence imaging [11–14].

The in-plane diffusion of excitons in QW is a complicated process involving excitonic propagation according to its thermal energy and scattering processes like phonon scattering and interface-roughness scattering. Despite the fact that the exciton–phonon scattering is enhanced by the confinement imposed by the QW [15], the interface-roughness scattering is still of particular importance in a realistic QW sample. Although modern epitaxy techniques, like molecular-beam epitaxy and metal–organic vapour phase epitaxy, can produce high-quality samples by depositing the atoms or molecules layer by layer, fluctuations with an atomic-size amplitude are inevitable on the interface between two materials. This interface roughness induces fluctuations of the potential along the QW, thus strongly influencing the excitonic diffusion. Indeed, previous experiments have confirmed that the exciton diffusivity of QW samples grown with interruption, which results in an improved interface quality, is significantly larger than that from samples grown without interruption [16]. However, although the impacts of other scattering processes on diffusion can be quantitatively studied in experiments by, for example, varying the sample temperature, the influence of the interface-roughness scattering is hard to examine quantitatively since the detailed structural information of the interfaces of a particular QW sample is typically unavailable.

Theoretical investigations of the excitonic transport are based on the Boltzmann equation in the framework of a semiclassical approach. To solve this equation and obtain the diffusivity of QW excitons, the relaxation-time assumption has been used [17, 18]. In this assumption, the influence of the scattering events on the transport process is described by relaxation times that are related to the rates of the scattering mechanisms. Another option is to perform Monte Carlo simulation [19]. In such calculations, the rates of several scattering mechanisms are calculated previously and the microscopic motion of each exciton is simulated to obtain the macroscopic property of the system. Since this method is based on a detailed description of individual excitons, it applies to both thermal and non-thermal excitons. In this paper, we report a detailed investigation of the influence of interface-roughness scattering on excitonic diffusion in QWs by Monte Carlo simulation. In this calculation, we take ZnSe QW as a model system. As an important candidate for short-wavelength applications, ZnSe-based structures have attracted much attention in recent years. Comparing to that for GaAs, the epitaxy deposit technique is less developed for II–VI systems, including ZnSe. Consequently, the ZnSe QW generally has a lower interface quality than GaAs systems. Thus, the influence of interface roughness on the excitonic process is anticipated to be more pronounced in ZnSe QW. From the simulation, we show quantitatively how the structure of the interfaces and the well width do influence the excitonic diffusion in QWs.

2. Interface roughness scattering

A semiconductor QW is composed of a well layer of one material sandwiched between two layers of another material with a larger energy bandgap. The potential changes abruptly at the interface between the two materials, providing a vertical confinement of the carriers in the QW. In reality, the interfaces cannot be absolutely abrupt due to the limitations of the growth techniques as well as the inter-diffusion of the two materials. The interface roughness can be regarded as a fluctuation of the QW thickness. This induces the fluctuation of the potential field of carriers along the QW plane, which scatters the carriers as they move in the well.

The method for calculating the scattering process of carriers by interface roughness has been established by Ando *et al* [20]. Generally, two parameters are used to characterize the structure of the interface, a height Δ and a length Γ. The former is the amplitude of the well-

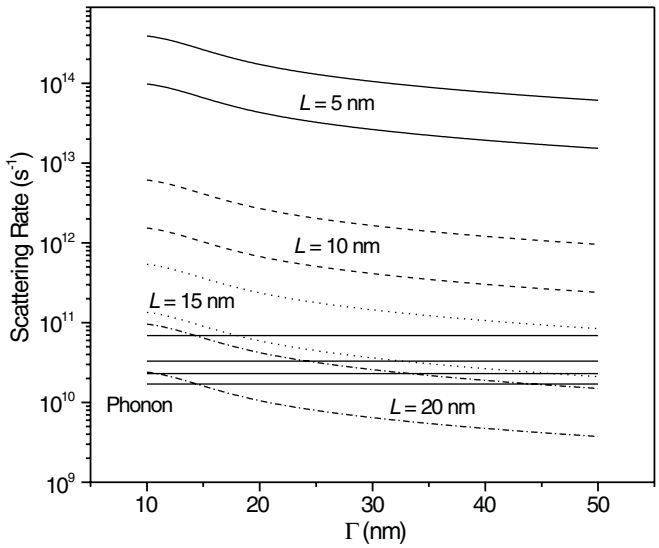

Figure 1. Scattering rates of interface roughness as a function of the correlation length, Γ, calculated for ZnSe QWs. The values of the well width are 5 (full), 10 (broken), 15 (dotted) and 20 nm (chain), respectively. For each pair of curves for a particular value of the well width, the upper curve corresponds to $\Delta = 0.566$ nm (two monolayers), while the lower one corresponds to $\Delta = 0.283$ nm (one monolayer). The horizontal full lines are the calculated phonon-scattering rates at a sample temperature of 10 K for different values of the well width (5, 10, 15 and 20 nm from top to bottom).

thickness fluctuation while the latter is the correlation length describing the lateral size of the fluctuations. By assuming a Gaussian correlation function of the well-width fluctuation and using the Fermi golden rule, the rate for an exciton with wavevector K to be scattered with a scattering angle θ is [17]

$$r(\theta) = \frac{1}{2}\pi^4\hbar\Gamma^2\Delta^2(m_e + m_h)\left(\frac{4}{La_B}\right)^6(1-\cos\theta)\exp(-\Gamma^2q^2/4)\left(\frac{\gamma_c}{m_e} - \frac{\gamma_v}{m_h}\right)^2. \tag{1}$$

Here, m_e and m_h are the effective mass of the electron and hole, respectively. L is the well width and a_B is the Bohr radius of the exciton. γ_c and γ_v are given by

$$\gamma_{c(v)} = \left[\left(\frac{4}{a_B}\right)^2 + \left(\frac{m_{h(e)}q}{m_e + m_h}\right)^2\right]^{-3/2}. \tag{2}$$

q is the change of the wavevector during scattering and is related to the value of the wavevector of the exciton by $q = 2K\sin(\theta/2)$.

With these formulae, we calculate the integrated scattering rate of interface roughness with different parameters, as shown in figure 1. This is obtained by integrating equation (1) over θ from 0 to 2π. The material parameters from ZnSe used in the calculations are $m_e = 0.16$ and $m_h = 0.70$. The energy of the exciton is set to the thermal energy, k_BT, at a temperature $T = 10$ K. The rates for samples with well widths of 5, 10, 15 and 20 nm are shown. A pronounced decrease in the scattering rate with increasing well width is found, showing that in the samples with larger well widths, the interface plays a less important role than it does in thin QWs. For each value of the well width, the variations of the rates as a function of Γ is calculated for two different values of Δ, 0.283 nm (one monolayer) and 0.566 nm (two monolayers). In each pair of curves shown in figure 1, the upper curve corresponds

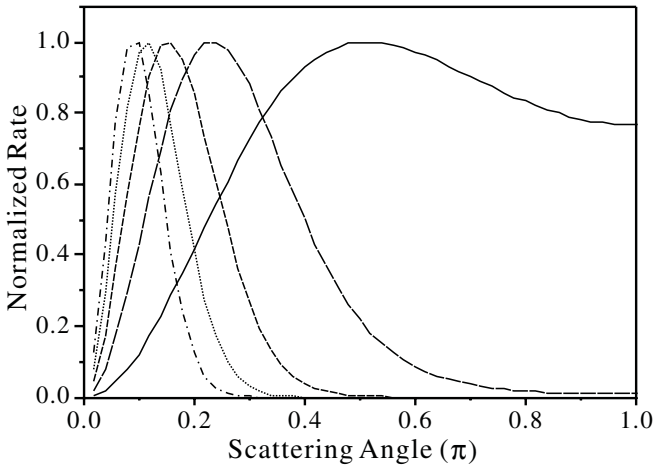

Figure 2. Angular dependence of the normalized scattering rate of interface roughness. The values of Γ are 10 (full), 20 (long-broken), 30 (short-broken), 40 (dotted) and 50 nm (chain), respectively.

to $\Delta = 0.566$. As anticipated, the larger Δ results in a higher rate of scattering. In all configurations, the scattering rate decreases with increasing Γ, i.e. with improving the interface quality. We also plot in the same figure the calculated phonon scattering rate of ZnSe QW for different values of the well width at a sample temperature of 10 K for comparison (the horizontal full lines). Since the optical phonon absorption and emission are negligible due to the low temperature and low exciton energy, respectively, the phonon-scattering rates are determined by the acoustic-phonon scattering processes, both absorption and emission. The plotted lines are the sum of the rates of these two processes. The material parameters used in the calculations are the deformation potentials of $D_h - D_e = 4.0$ eV, a sound speed of 4.65×10^3 m s^{-1}, both high and low frequency dielectric constants of 6.3 and 9.1, respectively, and a mass density of 5.28×10^3 Kg m^{-3}. Comparing to the interface-roughness scattering, the phonon scattering is obviously less sensitive to the well width. A change in well width from 5 to 20 nm corresponds to a decrease of the phonon-scattering rate from 6.9×10^{10} to 1.7×10^{10} s^{-1}. We see that, for narrow QWs, the interface roughness is the dominant scattering event at low temperatures. For wide QWs, the process is controlled by both phonon scattering and interface-roughness scattering.

Besides the scattering rate, the directional property of the scattering process is also important for excitonic diffusion. Being an elastic process, the interface-roughness scattering does not change the value of the exciton velocity but only its direction. A forward-scattering event only changes the direction of the velocity slightly and thus has a lesser impact on the diffusion. In contrast, the backward scattering reverses the direction and thus seriously influences the diffusion. In order to show this effect, we calculate the scattering rate of interface roughness as a function of the scattering angle by using equation (1). Figure 2 shows the calculated angular dependence of the scattering rate (normalized) for several values of Γ. In the case of $\Gamma = 10$ nm, the curve peaks at about $\pi/2$, indicating that the direction of the exciton velocity is most likely to be changed by an angle of $\pi/2$ after the scattering event. By increasing Γ, this angle becomes smaller and smaller, showing the forward-scattering feature in those samples with a larger Γ. This fact, together with the decrease in scattering rate by increasing Γ as shown in figure 2, implies that samples with larger Γ should have a large diffusivity of excitons. We note that this directional property is independent of Δ and L.

3. Monte Carlo simulation

The Monte Carlo method has been widely used for simulations of carrier dynamics in semiconductors [19, 21–24]. In this method, the motion of carriers in a semiconductor is simulated by assuming that the motion is composed of a series of free-flight processes terminated by scattering events. In this study, we use this method to simulate the real-space transport of excitons in the ZnSe QW plane at a sample temperature of 10 K and deduce the diffusivity of excitons as a function of the interface-roughness parameters.

Beside the interface-roughness scattering, the phonon scattering also influences excitonic diffusion. In our simulation, the phonon scattering mechanisms considered are acoustic-phonon emission and absorption. Since we study excitonic diffusion at low temperatures, the rate of optical-phonon absorption is negligible. The acoustic-phonon scattering rates are calculated by using the Fermi golden rule [25]. The result and rate of interface-roughness scattering calculated in the previous section are used as the input to the simulation. Since the scattering between excitons does not change the momentum of the whole system and, being a neutral particle, the screening effect of an exciton is negligible, the inter-exciton scattering is less important in determining the diffusion property and is thus not included in the simulation.

At the beginning of the simulation, a number of excitons are generated. Since the inter-exciton scattering is not included in the simulation, the number of excitons simulated does not influence the result itself but only its accuracy. In practice, a number of one million is found to be enough to ensure highly accurate ensemble averaging. The position of each exciton is selected randomly, while the overall distribution in space is a Gaussian function with a width of 500 nm. Recent experiments demonstrated that, when the excitons are generated with an energy larger than the thermal energy, the excitonic transport is strongly influenced by the energy relaxation [26]. Under this situation, transport cannot be described as a diffusion [27]. In our simulation, the excitons are generated with energy $E = k_{\mathrm{B}}T$ to exclude the influence of this hot-exciton effect. After being generated, each exciton undergoes a free-flight process. The duration of this process is determined by the total scattering rate. At the end of this process, one of the scattering mechanism is chosen to happen, according to the relative rates of all scattering mechanisms considered. In the case when the interface-roughness scattering event is selected to happen, one scattering angle is chosen randomly, according to the distribution shown in figure 2. In the case of phonon scattering, the final state of the exciton is calculated according to the energy and momentum of the phonon involved. After this scattering event, the exciton starts the next free-flight process, which will be terminated by the next scattering event. Such a free-flight/scattering process is repeated many times and the whole dynamics of each exciton is simulated.

Figure 3 shows an example of the temporal evolutions obtained of the exciton distribution. The locally generated excitons expand in space as time passes, as one anticipates for a diffusive motion. Such a spatiotemporal dynamics is well described by a diffusion equation characterized by a diffusivity. By analysing the evolution, we can get the diffusivity and study its variation with interface quality.

4. Results and discussion

At first, we study the dependence of the diffusivity on the correlation length of the interface roughness. Figure 4 shows the simulated result for ZnSe QW with a well width of 10 nm. The Δ is set to one (squares) and two (circles) monolayers, respectively. In both cases, the increase in diffusivity with Γ is obtained. Changing Γ from 10 to 50 nm, the diffusivity increases by about one order. Such a rapid increase is induced by both the decrease in the

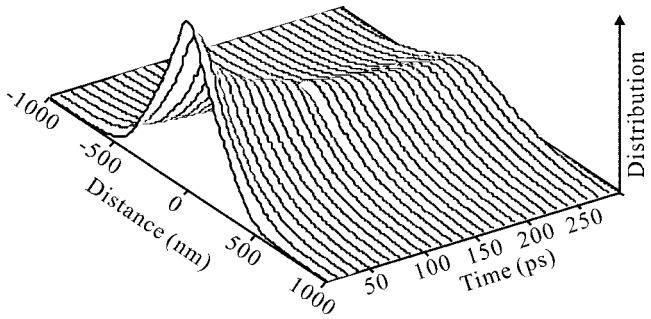

Figure 3. The temporal evolution of the exciton spatial distribution obtained by the simulation. The parameters used for this calculation are $L = 10$ nm, $\Delta = 1.5$ monolayer and $\Gamma = 30$ nm.

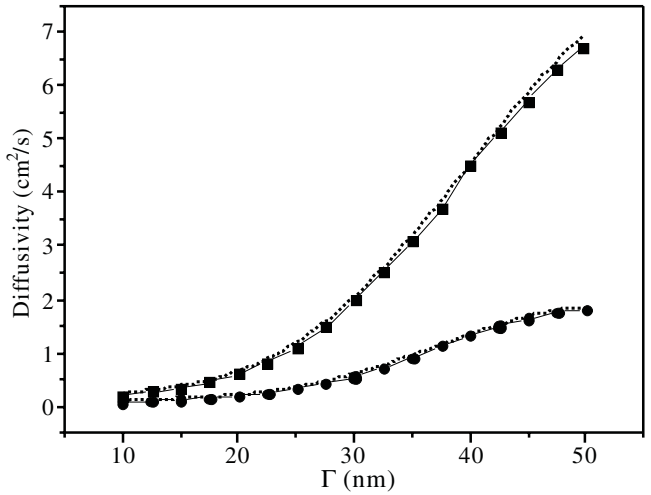

Figure 4. Excitonic diffusivity in ZnSe QW as a function of the correlation length (Γ) of the interface fluctuations. The well width is 10 nm. The amplitude of the fluctuation is one (squares) and two (circles) monolayers, respectively. The dotted curves are the corresponding results calculated by using the relaxation-time approximation as discussed in [17].

scattering rate and the change of the preferred scattering angle, as shown in figures 1 and 2. We note that a similar behaviour is also obtained for samples with other values of the well width. For comparison, we also performed similar calculations with the same set of parameters by using the relaxation-time approximation as described by Basu and Ray [17]. The results are shown in figure 4 as dotted curves. These two methods are equivalent in describing this process. We attribute the small difference between the results of the two methods to the fact that, in the relaxation-time approximation, the exciton energy distribution is described by a Boltzmann distribution while in the Monte Carlo simulation the initial exciton energy is defined as $k_{\mathrm{B}}T$, which is consistent with the laser excitation conditions used in typical experiments. Despite the equivalence shown here, we note that the Monte Carlo method is valid not only for this kind of equilibrium process: it can also be easily generalized to describe nonthermal exciton systems as well as more complicated situations with specific structures, since it is based on simulation of the microscopic processes of individual excitons. The relaxation-time approximation, however, is hard to use for nonthermal systems since the energy distribution is unknown.

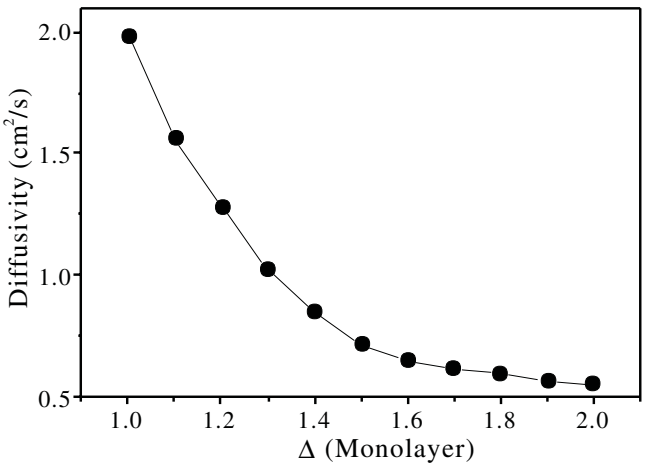

Figure 5. Excitonic diffusivity in ZnSe QW as a function of the fluctuation amplitude (Δ) of the interface. The well width is 10 nm and Γ is 30 nm.

Second, we calculate the excitonic diffusivity as a function of Δ. Since Δ describes the amplitude of the interface fluctuation, it has the unit of a monolayer. That is, at any particular location, Δ is an integer times the monolayer (0.283 nm). However, to describe the structure of the whole interface, the Δ used in the simulation is an average number. In practice, since the most frequently presented fluctuation is one or two monolayers, the average value of Δ is typically a number between one and two monolayers, depending on the interface quality. Figure 5 shows the calculated diffusivity as a function of Δ for a ZnSe QW sample with a well width of 10 nm and a Γ of 30 nm. Changing the Δ from one to two monolayers, the diffusivity drops by about three times.

We have shown that, in a realistic semiconductor QW sample, the interface quality has a dominant impact on the excitonic diffusivity. Furthermore, under the situation that the diffusivity is limited by interface roughness, which is the case for most samples, the well width is also an important parameter to control the diffusivity. It is obvious that, in wide QWs, the interface plays a less important role. With the same interface parameters, the scattering rate of interface roughness is significantly smaller in wide QWs. Figure 6 shows a quantitative description of the well-width dependence of the diffusivity. We find an exponential increase in diffusivity with well width in the range from 5 to 30 nm. We note that such a strong variation of the diffusivity with well width can be used to make a judgment on whether the excitonic diffusion is limited by the interface roughness or phonon scattering.

Although experimental data quantitatively describing the influence of interface structure on excitonic diffusion is still unavailable, there are measurements on excitonic diffusivity of ZnSe QW samples with unknown interface parameters. From time-integrated microphotoluminescence experiments, a diffusion length of about 600 nm has been deduced from ZnSe QW with well widths of 7.3 and 5 nm [28]. Taking an excitonic lifetime of 300 ps, this corresponds to a diffusivity of about 10 $cm^2\ s^{-1}$. Furthermore, recent time-resolved photoluminescence experiments shows a diffusivity of about 2 $cm^2\ s^{-1}$ for a ZnSe QW of 8 nm well width [29]. These numbers can be found in the simulation results with suitable interface-roughness parameters. This fact confirms partly the validity of the simulation. It also shows that the diffusion of excitons in a realistic QW sample is dominated by interface roughness.

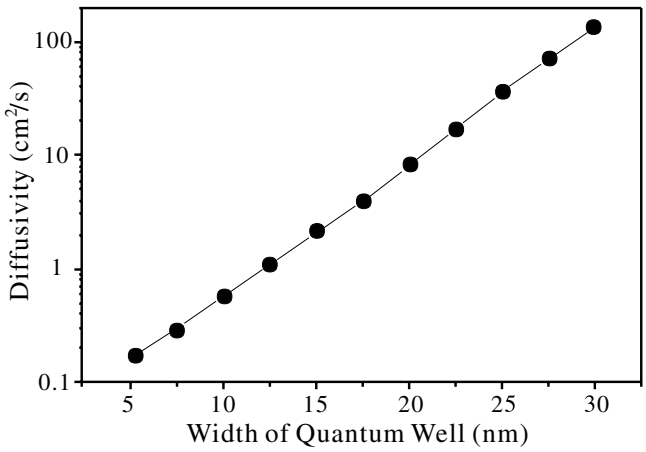

Figure 6. Excitonic diffusivity in ZnSe QW as a function of the well width (L). The parameters of the interface roughness used in this simulation are $\Delta = 1.5$ monolayers and $\Gamma = 30$ nm.

5. Conclusion

We study the excitonic diffusion in a semiconductor by the Monte Carlo method. The rates of interface-roughness scattering are calculated. It is found that, in a realistic QW sample with a typical well width and interface quality, the interface-roughness scattering is the dominant mechanism in limiting the diffusivity. We perform simulations of the excitonic dynamics and obtain the spatiotemporal dynamics of the exciton distribution function, from which the diffusivity is deduced. The diffusivity increases rapidly with increasing the correlation length of the interface fluctuation and with decreasing the amplitude of the fluctuation. In a typical QW sample in which the excitonic diffusion is limited by interface roughness, the diffusivity increases exponentially with increasing the width of the QW.

References

[1] Shah J 1996 *Ultrafast Spectroscopy of Semiconductors and Semiconductor Nanostructures* (Berlin: Springer) chapter 2
[2] Hegarty J, Goldner L and Sturge M D 1984 *Phys. Rev.* B **30** 7346
[3] Schwab H, Pantke K-H, Hvam J M and Klingshirn C 1992 *Phys. Rev.* B **46** 7528
[4] Schaefer A C, Erland J and Steel D G 1996 *Phys. Rev.* B **54** 11046
[5] Smith L M, Wake D R, Wolfe J P, Levi D, Klein M V, Klem J, Henderson T and Morkoç H 1988 *Phys. Rev.* B **38** 5788
[6] Achermann M, Nechay B A, Morier-Genoud F, Schertel A, Siegner U and Keller U 1999 *Phys. Rev.* B **60** 2101
[7] Nechay B A, Siegner U, Morier-Genoud F, Schertel A and Keller U 1999 *Appl. Phys. Lett.* **74** 61
[8] Hillmer H, Forchel A, Hansmann S, Morohashi M, Lopez E, Meier H P and Ploog K 1989 *Phys. Rev.* B **39** 10901
[9] Hillmer H, Forchel A and Tu C W 1992 *Phys. Rev.* B **45** 1240
[10] Akiyama H, Matsusue T and Sakaki H 1994 *Phys. Rev.* B **49** 14523
[11] Moehl S, Zhao H, Dal Don B, Wachter S and Kalt H 2003 *J. Appl. Phys.* **93** 6265
[12] Chao L-L, Gargill G S III, Snoeks E, Marshall T, Petruzzello J and Pashley M 1999 *Appl. Phys. Lett.* **74** 741
[13] Monte A F G, da Silva S W, Cruz J M R, Morais P C and Chaves A S 2000 *Phys. Rev.* B **62** 6924
[14] Pulizzi F, Christianen P C M, Maan J C, Eshlaghi S, Reuter D and Wieck A D 2002 *Phys. Status Solidi* b **190** 641
[15] Zhao H, Wachter S and Kalt H 2002 *Phys. Rev.* B **66** 085337
[16] Hillmer H, Forchel A, Sauer R and Tu C W 1990 *Phys. Rev.* B **42** 3220

[17] Basu P K and Ray P 1991 *Phys. Rev.* B **44** 1844
[18] Hai G Q, Studart N, Peeters F M, Koenraad P M and Wolter J H 1996 *J. Appl. Phys.* **80** 5809
[19] Jacoboni C and Lugli P 1989 *The Monte Carlo Method for Semiconductor Device Simulation* (New York: Springer)
[20] Ando T, Fowler A B and Stern F 1982 *Rev. Mod. Phys.* **54** 437
[21] Lugli P and Goodnick S M 1987 *Phys. Rev. Lett.* **59** 716
[22] Artaki M and Hess K 1988 *Phys. Rev.* B **37** 2933
[23] Zhao H, Wang Y, Xu Z and Xu X 1999 *J. Phys.: Condens. Matter* **11** 2145
[24] Shchegrov A V, Birkedal D and Shah J 1999 *Phys. Rev. Lett.* **83** 1391
[25] Takahashi Y 1996 *Phys. Rev.* B **53** 7322
[26] Zhao H, Moehl S and Kalt H 2002 *Phys. Rev. Lett.* **89** 097401
[27] Zhao H, Moehl S and Kalt H 2002 *Appl. Phys. Lett.* **81** 2794
[28] Zhao H, Moehl S, Wachter S and Kalt H 2002 *Appl. Phys. Lett.* **80** 1391
[29] Zhao H, Dal Don B, Moehl S, Kalt H, Ohkawa K and Hommel D 2003 *Phys. Rev.* B **67** 035306